MATERIALS PHYSICS AND MECHANICS RESEACH ARTICLE

Submitted: April 8, 2023 Revised: April 30, 2023 Accepted: April 4, 2024

Studies of trapezoidal panels under thermo-mechanical load: a nonlinear dynamic analysis

E. Kumari [1] ✉, **S. Lal** [2],

[1] MBM University, Jodhpur, India

[2] Rajasthan Technical University, Kota, India

✉ emarti.me@mbm.ac.in

ABSTRACT

Large amplitude flexural and vibration behavior of trapezoidal panels with sixteen node degenerated shell element are studied under thermo-mechanical load. The finite element formulation has been done considering the first-order shear deformation theory with incorporation of Von Karman's geometric nonlinearity, and the governing equations are solved using energy and conservation time integration scheme (combination of trapezoidal and three-point Euler backward method). The efficacy of the method is checked for nonlinear static and dynamic responses of both trapezoidal plate and curved panel. The effect of cord to span ratio (c/a), radius to span ratio (R/a), boundary conditions and stacking sequence on the nonlinear dynamic response of trapezoidal panels are also investigated under thermo-mechanical load. Moreover, new results for nonlinear dynamic response of trapezoidal panels under step thermal load with and without radial pressure are also presented and that will be important outcomes for the scientific community.

KEYWORDS

trapezoidal panels • finite element method • laminated composite • thermo-mechanical • nonlinear dynamic

Citation: Kumari E, Lal S. Studies of trapezoidal panels under thermo-mechanical load: a nonlinear dynamic analysis. *Materials Physics and Mechanics*. 2024;52(2): 90–105.
http://dx.doi.org/10.18149/MPM.5222024_10

Introduction

The laminated trapezoidal panels widely used in the various industries like aeronautical (wing panels, tail panels), ship hulls, automobile and defence industries etc., due to its flexible, high strength to weight ratio, and superior corrosion resistance. This type of thin-wall structures are subjected to step thermal and mechanical load, hence the nonlinear dynamic behaviour of trapezoidal flat and curved panels is an important matter of concern to design sustainable structures. The studies of nonlinear dynamic response of laminated trapezoidal panels under step thermal load with and without mechanical load is very important, hence it is investigated.

Srinivasan and Babu [1] investigated the free vibration and flutter characteristics of laminated quadrilateral plates. The transverse vibrational frequencies and mode shapes characteristics of symmetric trapezoidal plates were analysed by implementing the superposition method [2]. Ng and Das [3] studied the linear free vibration and buckling behaviour of skew plates under in-plane forces by applying Galerkin's variational method. The linear vibration frequencies of composite triangular and trapezoidal shells was examined by employing shallow shell theory with Ritz method [4]. Han and Petyt [5,6] studied the linear vibration behaviour of composite plates of rectangular shape using *p*-version FEM (Finite Element Method) under no load and harmonic plane wave incident normal to plate surface; respectively. Vibration characteristics of continuous rectangular plates were analysed by using a discrete method [7]. Kumar *et al*. [8] elaborated the linear free vibrational behaviour of composite skew panels employing FEM with high order shear deformation based on the C_0 continuity.

Malekzadeh [9] investigated large amplitude free vibration characteristics of laminated skew thin plates by employing differential quadrature (DQ) method.

Gupta and Sharma [10] calculated the frequencies of clamped-simply supported trapezoidal plates having linearly varying thickness in the presence of thermal gradient by applying Rayleigh-Ritz method. Nguyen-Minh *et al*. [11] illustrated the free vibration characteristics of trapezoidal and sinusoidal corrugated panels using homogenization method with first order shear deformation theory. It was considered a cell-based smoothed Mindlin plate element for linear dynamic analysis. Rout *et al*. [12] studied the free vibration characteristics of doubly curved composite panels under thermal loading by employing FEM with consideration of higher-order shear deformation theory. Liu *et al*. [13] conducted experiments on six different shape aluminium plates and applied unified coordinate transformation method with Lagrange interpolation method to study the in-planer free vibration behaviour of arbitrarily shaped plates. Authors compared the analytical (two-dimensional spectral-Chebyshev polynomial) and experimental results with available numerical results for clamped and cantilever boundary conditions. Niu and Yao [14] carried out the linear and nonlinear vibrational analysis of composite tapered flat graphene platelet and curved panels under transverse excitations. Li and Cheng [15] studied the vibration characteristics pre-twisted rotation blades using shallow shell theory. It was considered the centrifugal force and Coriolis acceleration due to rotation of blade and observed the effect of spring stiffness variation, thickness variation of cantilever plate.

Dou *et al*. [16] investigated the shear buckling behaviour of corrugated isotropic plates using FEM based ANSYS R113.0 software. Franzoni *et al*. [17] experimentally studied the buckling behaviour of unstiffened laminated cylindrical shells; and compared the presented experimental results with numerical results obtained by ABQUAS 6.16. Magnucka-Blandzi [18,19] formulated the multi-layered beam and trapezoidal plate using Hamilton's principle to study the stability and vibrational behaviour of thin-walled structure, and compared the presented analytical results with numerical results. Watts *et al*. [20] used the element free Galerkin method to investigate the dynamic instability characteristics of shear deformable trapezoidal plate under non-uniform compressive loads. It was derived the governing equations by employed the Hamilton's principle and Mathieu-Hill type ordinary differential equations and solved by Bolotin's method to analyse the dynamic instability. Linear and nonlinear static and dynamic responses of folded structures, rectangular and trapezoidal curved panels were investigated [21–27] by using the FEM based first-order shear deformation theory with incorporating the von-Karman's kinematic geometric nonlinearity. The linear vibration behaviour of functionally graded plates resting on elastic foundation was studied by Kumar *et al*. [28] using higher-order shear deformation theory. Recently, in [29–32] it was investigated the stability characteristics of structures in the presence of thermal environment.

From the literature review, it is observed that the large amplitude flexural vibration behaviour of composite trapezoidal panels is scarce. Therefore, the dynamic characteristic of trapezoidal panels subjected to thermo-mechanical loading is illustrated here. In this communication, the authors employed the finite element method using a degenerated shell element to study the large amplitude flexural vibration behaviour of laminated composite trapezoidal panels under mechanical load in the presence of a thermal environment.

Mathematical Modelling

FEM Formulations

A schematic representation of shell element geometry is presented in Fig. 1, it is having sixteen nodes and five degrees of freedom at each node (u_1^k, u_2^k, u_2^k, α_k and β_k) is used here to modelling the composite trapezoidal panels. The global geometrical coordinates x_i, *I* = 1, 2, 3 and displacement components u_i, *i* = 1, 2, 3 along the unit vectors V_1^k, V_2^k and V_n^k as represented in the Fig. 1 [33].

$$x_i = \sum_{k=1}^{16} N_k\, x_i^k + \frac{t}{2}\sum_{k=1}^{16} hN_k\, {}^tV_{ni}^k, \quad (1)$$

$$u_i = \sum_{k=1}^{16} N_k\, u_i^k + \frac{t}{2}\sum_{k=1}^{16} hN_k V_{ni}^k, \quad (2)$$

where, N_k is an interpolation function associated with the node k = 1, 16; x_i^k is the global coordinates of the node *k*, *i* = 1, 2, 3; ${}^tV_{ni}^k$ is normal to the shell mid-surface at node k; $V_{ni}^k = {}^tV_{ni}^k - {}^0V_{ni}^k$ stores the addition in the direction cosines of ${}^0V_{ni}^k$.

$$\Delta V_n^k = -{}^tV_2^k\alpha_k + {}^tV_1^k\beta_k \quad (3)$$

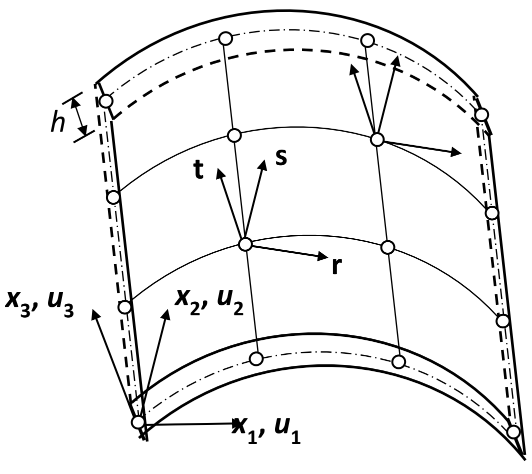

Fig. 1. Schematic diagram of 16-node shell element

The alteration in the direction cosines of the shell element (ΔV_n^k) shall be demonstrated as a nodal rotations (α_k and β_k) about two unit vectors ${}^tV_1^k$ and ${}^tV_2^k$ at the time *t* as [33–35].

The strain tensors ($\varepsilon_{ij} = e_{ij} + \eta_{ij}$) may be written as linear strains (e_{ij}) and nonlinear strains (η_{ij}) in terms of displacement components (u_i, *i* = 1, 2, 3):

$$e_{ij} = \frac{1}{2}(u_{i,j} + u_{j,i}) \text{ and } \eta_{ij} = \frac{1}{2}u_{k,i}u_{k,j};\ i, j, k = 1, 2, 3. \quad (4)$$

Firstly, the strain components are determined by direct interpolation at the Gaussian points, and it is called direct strains ε_{ij}^{DI}. Thereafter, the shear strains & direct strain components are further interpolated at the trying points to eliminate the spurious membrane and computed the assumed strains may be written as:

$$\varepsilon_{ij}^{AS}(r,s) = \sum_{k=1}^{n_{ij}} N_k^{ij}(r,s)\varepsilon_{ij}^{DI}(r,s), \tag{5}$$

here, $N_k^{ij}(r,s)$ represents the interpolation functions or shape functions (polynomials in isoparametric coordinate systems *r* and *s*) associated with the strain component ε_{ij}at trying point *k* and n_{ij} is the number of trying points (adopted from Bathe [33]).

The σ_{ij} is thermo-elastic stress component in a lamina which having ply-orientation (θ) with unit vector V_1^k will be written as:

$$\begin{Bmatrix} \sigma_{11} \\ \sigma_{22} \\ \sigma_{33} \\ \sigma_{23} \\ \sigma_{13} \\ \sigma_{12} \end{Bmatrix} = \begin{bmatrix} \bar{Q}_{11} & \bar{Q}_{12} & 0 & 0 & 0 & \bar{Q}_{16} \\ \bar{Q}_{21} & \bar{Q}_{22} & 0 & 0 & 0 & \bar{Q}_{26} \\ 0 & 0 & 0 & 0 & 0 & 0 \\ 0 & 0 & 0 & \bar{Q}_{44} & \bar{Q}_{45} & 0 \\ 0 & 0 & 0 & \bar{Q}_{54} & \bar{Q}_{55} & 0 \\ \bar{Q}_{61} & \bar{Q}_{62} & 0 & 0 & 0 & \bar{Q}_{66} \end{bmatrix} \begin{Bmatrix} \varepsilon_{11} - \alpha_{11}\Delta T \\ \varepsilon_{22} - \alpha_{22}\Delta T \\ \varepsilon_{33} \\ \varepsilon_{23} \\ \varepsilon_{13} \\ \varepsilon_{12} - \alpha_{12}\Delta T \end{Bmatrix} \tag{6}$$

where, $\bar{Q}_{ij}$is the plane stress-reduced stiffness matrix of the laminates at *h* from the natural *x*-axis may be written by:

$\bar{Q}_{11} = Q_{11} cos^4\theta + 2(Q_{12} + 2Q_{66}) sin^2\theta\, cos^2\theta + Q_{22} sin^4\theta,$
$\bar{Q}_{12} = (Q_{11} + Q_{22} - 4Q_{66}) sin^2\theta\, cos^2\theta + Q_{12}(sin^4\theta + cos^4\theta),$
$\bar{Q}_{22} = Q_{11} sin^4\theta + 2(Q_{12} + 2Q_{66}) sin^2\theta\, cos^2\theta + Q_{22} cos^4\theta,$
$\bar{Q}_{16} = (Q_{11} - Q_{12} - 2Q_{66}) sin\,\theta\, cos^3\theta + (Q_{12} - Q_{22} + 2Q_{66}) sin^3\theta\, cos\,\theta,$
$\bar{Q}_{26} = (Q_{11} - Q_{12} - 2Q_{66}) sin^3\theta\, cos\,\theta + (Q_{12} - Q_{22} + 2Q_{66}) sin\,\theta\, cos^3\theta,$
$\bar{Q}_{66} = (Q_{11} + Q_{22} - 2Q_{12} - 2Q_{66}) sin^2\theta\, cos^2\theta + Q_{66}(sin^4\theta + cos^4\theta),$
$\bar{Q}_{44} = Q_{44} cos^2\theta + Q_{55} sin^2\theta,\ \bar{Q}_{45} = (Q_{55} - Q_{44}) cos\,\theta\, sin\,\theta,$
$\bar{Q}_{55} = Q_{55} cos^2\theta + Q_{44} sin^2\theta,$

where, $Q_{11} = \frac{E_1}{1-\nu_{12}\nu_{21}};\ Q_{12} = \frac{\nu_{12}E_2}{1-\nu_{12}\nu_{21}};\ Q_{22} = \frac{E_2}{1-\nu_{12}\nu_{21}};\ Q_{66} = G_{12};\ Q_{44} = G_{23};\ Q_{55} = G_{13};$

α_{ij} is the transformation of thermal coefficients and it can be written by:

$\alpha_{11} = \alpha_L cos^2\theta + \alpha_T sin^2\theta;\ \alpha_{22} = \alpha_L sin^2\theta + \alpha_T cos^2\theta;\ \alpha_{12} = (\alpha_L - \alpha_T) cos\,\theta\, sin\,\theta.$

The E_1, E_2 and E_3 in above equations are young's modulus along longitudinal, transverse and normal directions respectively; G_{23}, G_{13} and G_{12} are shear modulus in the *2-3* plane, *1-3* plane and *1-2* plane respectively; $\nu_{23} = \nu_{13} = \nu_{12}$ is the Poisson's ratio; and α_L and α_T are thermal expansion coefficient along with the longitudinal and transverse direction; $\Delta T = T - T_0$ is the change in temperature from room temperature T_0.

Anisotropic case reduced to isotropic: $E_1 = E_2 = E_3 = E$; $\nu_{12} = \nu_{13} = \nu_{23} = \nu$ and $\alpha_L = \alpha_T = \alpha$.

Governing equation of motion for nonlinear dynamic analysis

The nonlinear equation of motion for dynamic analysis of isotropic and laminated composite trapezoidal panels under thermo-mechanical loading condition can be written as:

$$[M]\{\ddot{\delta}\} + [K_L + K_{NL1}(\delta) + K_{NL2}(\delta,\delta)]\{\delta\} = \{F_M\} + \{F_T\}. \tag{7}$$

Here, $[M]$ is the mass matrix; $[K_L]$ is the linear stiffness matrix; $[K_{NL1}]$ and $[K_{NL2}]$ are the nonlinear stiffness matrix; $\{\delta\}$ and $\{\ddot{\delta}\}$are the displacement and acceleration vector of degrees of freedom; $\{F_M\}$ and $\{F_T\}$ are the nodal load vectors due to radial pressure and thermal load; respectively.

Solution procedure

Nonlinear static analysis. The equation (7) will be employed to investigate the linear and nonlinear bending and vibrational analysis by neglecting the appropriate terms.

The governing equation for nonlinear bending analysis may be expressed as:

$$[K_L + K_{NL1}(\delta) + K_{NL2}(\delta,\delta)]\{\delta\} = \{F_M\} + \{F_T\}. \quad (8)$$

The Newton Raphson iterative scheme is used to solve the Eq. (8) for nonlinear static analysis of trapezoidal panels.

Residual force:

$$\{\Delta F^i\} = [K_L + K_{NL1}(\delta^i) + K_{NL2}(\delta^i,\delta^i)]\{\delta^i\} - \{F_M\} - \{F_T\}, \quad (9)$$

$$[K_T^i]\{\Delta\delta^{i+1}\} = \{\Delta F^i\}, \quad (10)$$

$$\{\delta^{i+1}\} = \{\delta^i\} + \{\Delta\delta^{i+1}\}, \quad (11)$$

where, $[K_T]$ is tangent stiffness matrix and "*i*" (i = 1, 2, 3, ...) is the number of iterations.

The iteration process is repeated until the difference between $\{\delta^i\}$ and $\{\delta^{i+1}\}$ becomes smaller than error tolerance (ε = 0.001) as discussed by Maleki and Tahani [37]. In this investigation an error criteria is taken by:

$$\sqrt{\frac{\sum_{J=1}^{NP}\left|\delta_J^{i+1} - \Delta\delta_J^{i+1}\right|^2}{\sum_{J=1}^{NP}\left|\Delta\delta_J^{i+1}\right|^2}} \le \varepsilon, \quad (12)$$

where N_P is number of unknowns.

Linear vibration analysis. Linear free vibration frequencies of trapezoidal panel are determined by neglecting appropriate terms in Eq. (7), equation of motion is written as follows:

$$[M]\{\ddot{\delta}\} + [K_L]\{\delta\} = \{0\}. \quad (13)$$

Here, displacement $\{\delta\}$ vector is assumed to be function of simple harmonic motion$\{\delta\} = A\sin\omega_i t$; $\{\ddot{\delta}\} = -A\omega_i^2 \sin\omega_i t$; i = 1,2,3.....n (n = degree of freedom of the panel). By using Eq. (13) calculated the natural frequencies of the trapezoidal panels.

Nonlinear dynamic analysis. The nonlinear dynamic analysis of trapezoidal panel is obtained by solving Eq. (7) with the defined initial conditions.

$$\{\delta(0)\} = \{a\} \text{ and } \{\dot{\delta}(0)\} = \{b\}. \quad (14)$$

The energy and momentum conservation implicit time integration method [30] has been used here to solve the equation of motion (7) for the nonlinear dynamic response of trapezoidal panels under thermo-mechanical load.

The velocity and acceleration at each time step ($t + \Delta t$) may be written as:

$$\dot{\delta}_{(t+\Delta t)} = \frac{1}{\Delta t}\delta_{(t)} - \frac{4}{\Delta t}\delta_{(t+\Delta t/2)} + \frac{3}{\Delta t}\delta_{(t+\Delta t)}, \quad (15)$$

$$\ddot{\delta}_{(t+\Delta t)} = \frac{1}{\Delta t}\dot{\delta}_{(t)} - \frac{4}{\Delta t}\dot{\delta}_{(t+\Delta t/2)} + \frac{3}{\Delta t}\dot{\delta}_{(t+\Delta t)}. \quad (16)$$

By substituting Eqs. (15), (16) into Eq. (7), we obtain:

$$\left[\frac{9}{\Delta t^2}M + K_T\right]\Delta\delta^i = F_{(t+\Delta t)} - (K_L + K_{NL})\delta_{(t+\Delta t)}^{(i-1)}\frac{1}{\Delta t}\dot{\delta}_{(t)} - $$
$$-M\left[\frac{9}{\Delta t^2}\delta_{(t+\Delta t)}^{(i-1)} - \frac{12}{\Delta t^2}\delta_{(t+\Delta t/2)} + \frac{3}{\Delta t^2}\delta_{(t)} - \frac{4}{\Delta t}\dot{\delta}_{(t+\Delta t/2)} + \frac{1}{\Delta t}\dot{\delta}_{(t)}\right]. \quad (17)$$

Incremental displacement is updated at each sub-step using Eq. (11).

Results and Discussion

Geometrical model design

The schematic diagram of the trapezoidal (symmetric and unsymmetrical) flat and curved panels is shown in Fig. 2 with fiber orientation.

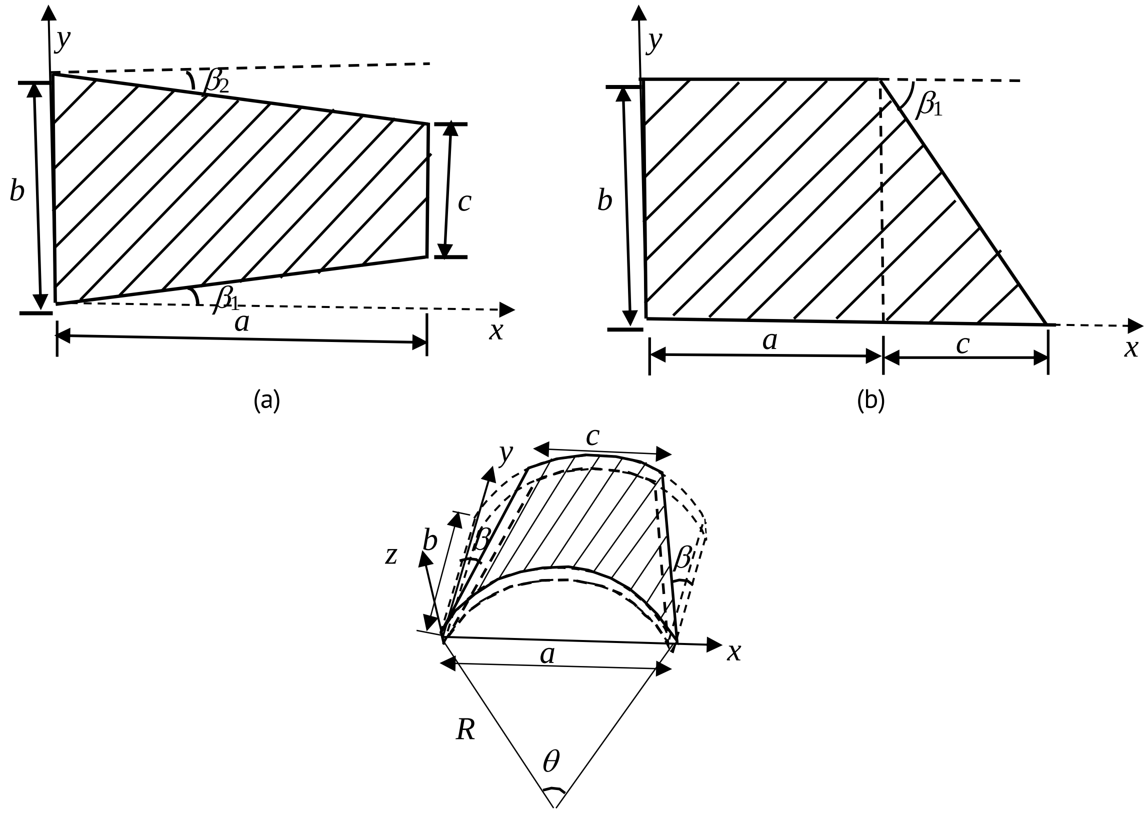

(c)

Fig. 2. Schematic representation of geometry with fibre-orientation of laminated (a) symmetric trapezoidal plate, (b) unsymmetrical trapezoidal plate, and (c) symmetric trapezoidal curved panel

Boundary conditions

The following boundary conditions are considered which are expressed in Table 1.

Table 1. Boundary conditions of various cases and their degree of freedom

S. No.	Boundary conditions	Degree of freedom restrained
1	Simply supported (*SSSS*)	
	Case 1	$u_l = u_t = u_3 = 0$; *along all edges*
	Case 2	$u_l = u_3 = \beta_t = 0$; at $x = 0, a$ and; $u_t = u_3 = \alpha_l = 0$; at $y = 0, b$
2	Clamped (*CCCC*)	$u_l = u_t = u_3 = \alpha_l = \beta_t = 0$; along all edges
3	CSCS	$u_l = u_t = u_3 = \alpha_l = \beta_t = 0$ at $y = 0, b$; $u_l = u_3 = \beta_t = 0$ at $x = 0, a$
4	*SCSF*	$u_l = u_t = u_3 = 0$; at $x = 0, a$; $u_l = u_t = u_3 = \alpha_l = \beta_t = 0$ at $y = 0$

Model validation

The following material properties of isotropic and laminated composite trapezoidal panels have been used to solve the equations:

1) For the Isotropic panels: $E = 1 \times 10^6$ N/m^2, $\nu = 0.3$, $\rho = 1.0$ kg/m^3, $\alpha = 1 \times 10^{-6}$/°C.

2) For the Laminated composite panels: $E_1 = 53.8$ GPa, $E_2 = E_3 = 17.9$ GPa, $G_{23} = G_{13} = G_{12} = 8.68$ GPa, $\nu_{23} = \nu_{13} = \nu_{12} = 0.25$, $\rho = 1600$ kg/m^3, $\alpha_L = 6.3 \times 10^{-6}$/°C, $\alpha_T = 20.5 \times 10^{-6}$/°C, where, E_1, E_2, and E_3 denoted for young's modulus along longitudinal, transverse and normal direction; G_{23}, G_{13} and G_{12} are presented the shear modulus in $y - z$ plane, $x - z$ plane and $x - y$ plane respectively; ν_{23}, ν_{13} and ν_{12} are the Poisson's ratios; ρ is the density of used material; α_L and α_T are represents the thermal expansion along longitudinal and transverse directions; respectively.

Convergence Study

Linear bending and vibration analysis. First, examined the accuracy of developed FORTRAN code and evaluated the efficacy of degenerated sixteen node shell elements for linear vibration and bending analysis of symmetric and unsymmetrical trapezoidal flat panels as presented in the Tables 2 and 3, respectively.

The non-dimensional natural frequencies ($\varpi_i = (\omega_i a^2/\pi^2)\sqrt{\rho h/D}$; $i = 1{,}5$; ω_i is natural frequency in rad/sec; $D = Eh^3/12(1-\nu^2)$ is flexural rigidity of structure) of simply supported (case 1) and clamped isotropic symmetric trapezoidal are compared as given in Table 2 with available published results Watts *et al.* [20], Chopra and Durvasula [38] and Kitipornchai *et al.* [39] for various chord-to-span ratios (c/a = 0.2, 0.4, 0.6). Firstly, convergence study is performed for converge numerical results considering 2×2 and 4×4 mesh size. It is noticed that 4×4 mesh size results are matched very well with Galerkin method [38], Rayleigh-Ritz method [39] and meshless method [20]. Thereafter, percentage of errors are also examined for the isotropic ($\nu = 0.3$) symmetric trapezoidal flat panel (a/b = 1, and b/h = 100), and it is found that percentage of error is less than 0.1 and 0.2 % for fully clamped and simply supported panels, respectively. After mesh convergence, it is noticed that 4×4 mesh size is suitable for converged results. Moreover, also plotted the vibration mode shapes for an isotropic clamped symmetric trapezoidal flat panels (a/b = 1, b/h = 100, c/a = 0.6) and schematically shown in Fig. 3.

Then, the non-dimensional central deflection of simply supported (case 1) isotropic (ν=0.3) and laminated composite (cross-ply [0°/90°]$_S$ and angle-ply [45°/-45°]$_S$) moderately thick (a/h = 20) and thin (a/h = 100, 500) unsymmetrical trapezoidal (b/c = 1) flat panel are presented in Table 3 for different aspect ratios such as a/b = 1.0, 1.2, 1.4, 1.6, 1.8, and 2.0. The study is also compared the presented numerical and analytical results through Galerkin method published by Saadatpour and Azhari [36] for thin (a/h = 500) isotropic unsymmetrical trapezoidal plate. As concerned with error analysis, the root-mean-square error (RMSE) is evaluated and observed very small (0.0006120) as given in Table 3, it is concluded that the proposed model is given results with accuracy and found validated. So the author can use this model for future study. Moreover, the new results for static behaviour of cross-ply and angle-ply laminated unsymmetrical trapezoidal flat panels (a/b = 1, b/c = 1, β_2 = 0°, a/h = 20, 100, 500) under uniformly distributed load is presented in Table 3, considering following material properties: $E_1/E_2 = 25$, $G_{12} = G_{13} = 0.5E_2$, $G_{23} = 0.2E_2$, $\nu_{12} = 0.25$.

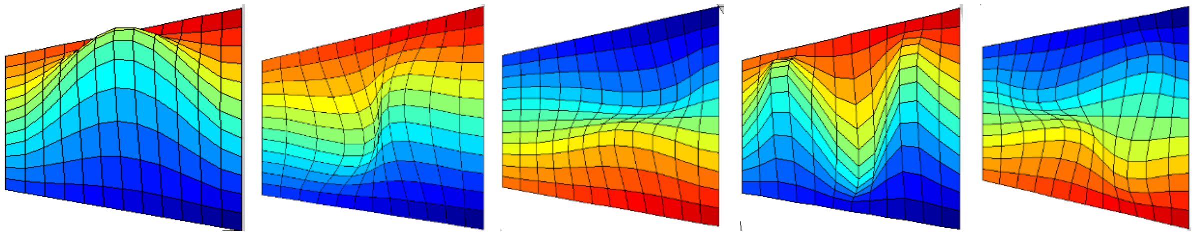

ϖ_1= 4.8063 ϖ_2= 8.4791 ϖ_3= 10.6156 ϖ_4= 14.2566 ϖ_5 = 14.7674

Fig. 3. First five vibrational mode shapes of an isotropic (ν = 0.3) clamped (*CCCC*) symmetric trapezoidal flat panel (*a*/*b* = 1, *b*/*h* = 100, *c*/*a* = 0.6)

Table 2. Non-dimensional natural frequencies ($\varpi_i = (\omega_i a^2/\pi^2)\sqrt{\rho h/D}; i = 1{,}5$) of a thin isotropic ($\nu$ = 0.3) trapezoidal plates (*a*/*b* = 1, *a*/*h* = 100)

Boundary conditions	***c/b***	**Normalized Natural frequency (ϖ)**		ϖ_1	ϖ_2	ϖ_3	ϖ_4	ϖ_5
SSSS (Case 1)	0.2	Present (FEM)	2 × 2	3.8344	8.2064	9.9940	14.8149	17.6728
			4 × 4	3.8151	8.0417	9.7639	13.6335	16.6335
		Chopra and Durvasula [38] (Galerkin Method)		3.8242	8.0707	9.7898	13.664	16.681
		Kitipornchai *et al.* [39] (Rayleigh-Ritz method)		3.8212	8.0728	9.7850	13.6748	16.6673
		Watts *et al.* [20] (Meshless method)		3.8291	8.0972	9.8081	13.7556	16.6910
	0.4	Present	2 × 2	3.1213	6.5321	8.5318	12.2655	13.8010
			4 × 4	3.1136	6.4522	8.3839	11.4693	13.3454
		Chopra and Durvasula [38]		3.1200	6.472	8.402	11.494	13.388
		Kitipornchai *et al.* [39]		3.1204	6.4727	8.3992	11.4933	13.3813
		Watts *et al.* [20]		3.1248	6.4861	8.4192	11.5220	13.4065
	0.6	Present	2 × 2	2.5971	5.7182	7.1772	10.8938	11.3703
			4 × 4	2.5934	5.6584	7.0794	10.6436	10.6798
		Chopra and Durvasula [38]		2.5977	5.67	7.091	10.656	10.710
		Kitipornchai *et al.* [39]		2.5977	5.6697	7.0904	10.6535	10.7076
		Watts *et al.* [20]		2.6004	5.6760	7.1053	10.6694	10.7324
CCCC	0.2	Present	2 × 2	7.4148	13.5881	17.1105	22.4752	27.3439
			4 × 4	7.2074	12.6375	14.8186	19.3755	23.0853
		Kitipornchai *et al.* [39]		7.2195	12.6609	14.8419	19.3154	23.0600
		Watts *et al.* [20]		7.2312	12.6798	14.9139	19.3719	23.1247
	0.4	Present	2 × 2	5.9607	10.1901	14.3788	18.2722	21.1821
			4 × 4	5.8630	9.9000	12.6365	15.5891	18.5473
		Kitipornchai *et al.* [36]		5.8721	9.9195	12.6607	15.6043	18.5838
		Watts *et al.* [20]		5.8839	9.9418	12.7294	15.6686	18.6473
	0.6	Present	2 × 2	4.8474	8.6882	11.7737	16.0929	16.9832
			4 × 4	4.8063	8.4791	10.6156	14.2566	14.7674
		Kitipornchai *et al.* [39]		4.8129	8.4954	10.6362	14.2726	14.8026
		Watts *et al.* [20]		4.8247	8.5200	10.6929	14.3362	14.8773

Percentage of error is less than 0.2 % for simply supported and fully clamped trapezoidal panels with Galerkin method [38], Rayleigh-Ritz method [39] and meshless method [20]

Table 3. The non-dimensional central deflection of simply supported (case 1) and for unsymmetrical trapezoidal plates (b/c = 1, β_2 = 0°)

a/b	**Isotropic (ν = 0.3) unsymmetrical trapezoidal plate** ($\bar{w} = 10^3 \times wD/q_0b^4$)							
	Moderately thick trapezoidal plate *a/h* = 20			**Thin trapezoidal plate *a/h* = 500**				
	Present study			**Present study**			[36]	RSME
	2 × 2	**4 × 4**	**6 × 6**	**2 × 2**	**4 × 4**	**6 × 6**	8 × 8	
1.0	4.1892	4.2415	4.2665	4.0592	4.0626	4.0628	4.062	1.35E-07
1.2	5.0202	5.0906	5.1206	4.8492	4.8219	4.8217	4.821	1.667E-07
1.4	5.7572	5.8423	5.8752	5.4944	5.4606	5.4631	5.466	2.52E-07
1.6	6.4005	6.4922	6.5260	6.0055	5.9756	5.9847	6.000	1.707E-05
1.8	6.9559	7.0441	7.0771	6.3918	6.3755	6.3942	6.437	0.0001602
2.0	7.4286	7.5052	7.5363	6.6743	6.6761	6.7059	6.787	0.0006120

	Laminated composite unsymmetrical trapezoidal plate ($\bar{w} = 10^3 \times wE_2h^3/q_0b^4$)					
	Cross-ply [0°/90°/90°/0°]			**Angle-ply [45°/-45°/-45°/45°]**		
	***a/h* = 20**	***a/h* = 100**	***a/h* = 500**	***a/h* = 20**	***a/h* = 100**	***a/h* = 500**
1.0	7.7473	6.8360	6.7981	6.4028	4.9037	4.7477
1.2	8.5401	7.1120	7.0457	8.3839	6.1497	5.9266
1.4	9.2115	7.1720	7.0509	10.4757	7.4711	7.1708
1.6	9.8598	7.1733	6.9657	12.5825	8.8101	8.4242
1.8	10.5214	7.1375	6.8353	14.6259	10.0658	9.8512
2.0	11.2070	7.0687	6.6712	16.5652	11.1619	10.5685

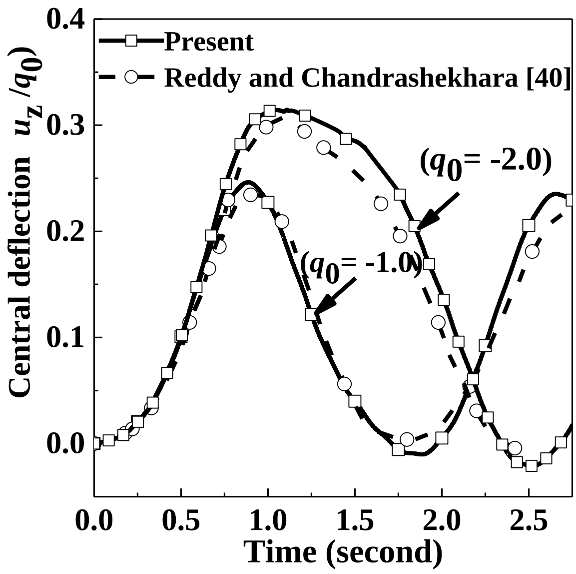

Fig. 4. Geometrical nonlinear dynamic response of simply supported (*Case* 4) laminated [90°/0°] double curved panel under external pressure (q_0 = -1 and -2)

Nonlinear dynamic response. The nonlinear dynamic response of cross-ply [90°/0°] spherical panel (a/b = 1, a/h = 100, h = 1, R/a = 10, R_1, = R_2 = R) under radial pressure (q_0 = -1, -2) is shown in Fig. 4 considering simply supported (case 2) boundary conditions. Here, employed the energy and momentum conservation implicit time integration scheme proposed by Bathe [41] to solve nonlinear governing equations. The linear vibration frequency (ω) of spherical panel is 3.697 radian/ second and time period (T_L) is 1.69921 second, time step is taken Δt = 0.01 second for geometric nonlinear dynamic response of spherical panel. The presented numerical results are validated with available published results of Reddy and Chandrashekhara [40] for nonlinear transient response of spherical panel, and it is noticed that the presented results have good combination with [40].

Results and Discussions

Linear vibration analysis of laminated panel. Next, the linear non-dimensional vibration frequencies ($\varpi_i = (\omega_i b^2/h)\sqrt{\rho/E_2}; i = 1{,}4$; ω_i is the circular frequency of composite panel) of simply supported (case 1) four-layer cross-ply $[0°/90°]_S$ and angle-ply $[45°/-45°]_S$ laminated composite unsymmetrical trapezoidal flat panels (b/c = 1, β_2 = 0°) is presented in Table 4 for moderately thick (a/h = 20) and thin (a/h = 100, 500) panels considering various aspect ratios for example a/b = 1.0, 1.2, 1.4, 1.6, 1.8 and 2.0. It is found that as increases the aspect ratio from a/b = 1.0 to 2.0, reduces the non-dimensional vibration frequencies (ϖ_i, i = 1, 4) for moderately thick (a/h = 20) and thin ($a/h \geq 100$) laminated trapezoidal panels.

Table 4. Non-dimensional fundamental frequency ($\varpi_i = (\omega_i b^2/h)\sqrt{\rho/E_2}; i = 1{,}4$) of simply supported (case 1) laminated composite unsymmetrical trapezoidal flat panels (b/c = 1, β_2 = 0°). Considering following material properties: E_1/E_2 = 25, G_{12} = G_{13} = 0.5E_2, G_{23} = 0.2E_2, ν_{12} = 0.25

a/h	*a/b*	Cross-ply $[0°/90°]_S$				Angle-ply $[45°/-45°]_S$			
		ϖ_1	ϖ_2	ϖ_3	ϖ_4	ϖ_1	ϖ_2	ϖ_3	ϖ_4
20	1.0	14.1929	25.9700	42.8389	48.4354	15.5091	30.4996	37.7022	48.1889
	1.2	13.4606	22.5612	39.2109	40.0881	13.5271	26.7153	32.2003	42.8126
	1.4	12.8997	20.2908	33.6547	36.6220	12.0772	23.2938	28.9447	38.2665
	1.6	12.3903	18.6256	29.3614	33.8671	11.0027	20.5636	26.6167	33.4631
	1.8	11.8984	17.2962	26.1164	31.4063	10.1949	18.4462	24.6956	29.2651
	2.0	11.4198	16.1731	23.5614	29.2088	9.5712	16.7754	22.9688	26.1155
100	1.0	15.1803	27.8593	53.9085	54.5452	17.8542	35.6111	47.0191	59.2310
	1.2	14.8428	24.8708	46.2017	53.5380	15.9418	32.3890	41.4478	54.9092
	1.4	14.7253	23.2124	40.7507	53.1872	14.4519	29.1601	38.2372	50.4681
	1.6	14.6297	22.1063	36.9479	52.7870	13.2918	26.3510	36.1501	45.9961
	1.8	14.5283	21.2615	34.1292	50.9178	12.4266	24.1580	34.5387	42.0954
	2.0	14.4272	20.5796	31.9784	46.7551	11.8054	22.4992	33.0892	39.1361
500	1.0	15.2259	27.9478	54.5568	54.8481	18.1603	36.0162	47.9907	60.1180
	1.2	14.9180	25.0153	46.6159	54.4707	16.2578	32.9332	42.4182	56.0401
	1.4	14.8607	23.4804	41.3221	54.4656	14.7703	29.8055	39.1841	51.7491
	1.6	14.8369	22.5338	37.6429	54.4527	13.6104	27.0374	37.1119	47.3796
	1.8	14.8015	21.8338	34.9227	52.9022	12.7531	24.8724	35.5583	43.5889
	2.0	14.7585	21.2691	32.9115	49.2364	12.1496	23.2509	34.2033	40.7276

Then, the non-dimensional fundamental vibration frequencies of five-layered laminated cross-ply and angle-ply composite trapezoidal curved (shown in Fig. 2(d)) panels (a/b = 1, a/h = 200 and R/a = 5) is given in Table 5 for various boundary conditions for example *CCCC*, *SSSS* case 2, *SCSF*. It is identified that by increasing the span to cord ratio (c/a = 0.2, 0.4, 0.6, 0.8, 1.0) reduces the vibration frequencies for different boundary conditions i.e. fully clamped (*CCCC*), simply supported (*SSSS* case 2), and *SCSF* boundary conditions. Trend of numerical results of cross-ply and angle-ply laminated composite trapezoidal curved panel is qualitatively similar, but the vibration frequency of cross-ply laminated panel (c/a = 0.2) is higher side compare to angle-ply composite panels for the case *CCCC*, *SCSF* boundary conditions; whereas, vibration frequency of regular shape (c/a = 1.0) panel is lower side for same case.

Table 5. Non-dimensional fundamental frequency ($\varpi_i = (\omega_i b^2/h)\sqrt{\rho/E_2}; i = 1{,}4$) of laminated composite symmetric trapezoidal curved (shown in Fig. 2(c)) panels (a/b = 1, a/h = 200 and R/a = 5)

Boundary conditions	c/a	Cross-ply [0°/90°/0°/90°/0°]				Angle-ply [45°/-45°/45°/-45°/45°]			
		ϖ_1	ϖ_2	ϖ_3	ϖ_4	ϖ_1	ϖ_2	ϖ_3	ϖ_4
CCCC	0.2	56.9120	65.0013	69.8813	89.0529	50.2041	61.5680	65.1301	85.0165
	0.4	54.2965	57.0587	62.7385	76.3326	47.2894	53.1792	57.5156	72.9480
	0.6	49.3405	51.9792	58.8479	65.5270	45.1230	45.4688	54.0883	64.1960
	0.8	42.2670	49.6560	56.7027	56.8583	39.7326	43.3319	52.6230	57.8579
	1.0	37.2144	46.6908	52.5165	55.2854	36.4844	41.1807	51.8634	54.3969
SSSS (case 2)	0.2	33.1823	53.1264	55.1647	73.3451	33.5581	52.1432	54.7831	73.3753
	0.4	27.9279	44.6200	48.3694	61.2444	28.0481	45.0114	47.7857	63.0979
	0.6	24.4497	40.9825	42.1846	54.9163	26.4124	37.4097	46.1345	54.3952
	0.8	23.7298	31.7367	42.7446	43.4487	27.5925	29.2541	46.0690	46.4634
	1.0	22.9628	24.3950	37.3112	43.9925	22.0271	29.4154	37.6981	43.1123
SCSF	0.2	50.2155	55.3062	63.2162	76.5029	47.6864	48.9190	56.8211	70.8112
	0.4	43.5048	53.5984	58.0567	63.5551	41.6769	45.8360	50.0730	58.3954
	0.6	36.3518	48.4946	51.2879	54.3916	32.4765	43.0491	46.0196	47.7162
	0.8	27.7035	39.8012	46.9176	50.5925	24.3752	38.1959	41.8596	44.3402
	1.0	21.9335	37.4441	38.4618	44.9045	20.7230	30.5711	39.8556	41.9476

Nonlinear dynamic response under thermal load. Next, the nonlinear static and dynamic responses of fully clamped (*CCCC*) cross-ply [0°/90°/0°/90°/0°] laminated composite trapezoidal curved panels (a/b = 1, a/h = 200, R/a = 5) under thermal load ΔT °C is plotted in Fig. 5 with outward and inward deformed shapes at time t = 0.563 second and 1.034 second, respectively.

The geometrical nonlinear dynamic responses: transverse central deflection (u_3/h) versus time is shown in Fig. 5(a) for clamped laminated trapezoidal panel for various cord-to-span ratios at thermal load (ΔT = 100 °C, at Room Temp. T_R = 20 °C) considering time step size Δt = 0.01 second. The natural frequency (ω_n) and time period (T_L) of these selected panels (a/b = 1, a/h = 200 and R/a = 5) with cord to span ratio c/a = 0.2, 0.4, 0.6, 0.8, 1.0 are ω_n = 4.8732, 4.6329, 4.4499, 3.8328 and 3.2067 radian/second; T_L = 1.2893, 1.3562, 1.412, 1.6392 and 1.9593 second; respectively. It is seen that as increases the cord-to-span ratio 0.2 to 1.0 then the time period of cycle T_L increases 1.2893 second to 1.9593 second. It is noticed that, the vibration amplitude increases with the increase in cord-to-span ratio. Moreover, nonlinear static response of trapezoidal panel for various cord to span ratios i.e. c/a = 0.2, 0.4, 0.6, 0.8, 1.0 at various temperatures ΔT = 0 to 1200 °C is shown in Fig. 5(b). It is noticed that central deflection (u_3/h) increases with increase in cord-to-span ratio, therefore thermal load carrying capacity is reduces. This occurs due to change in structural stiffness of trapezoidal panels.

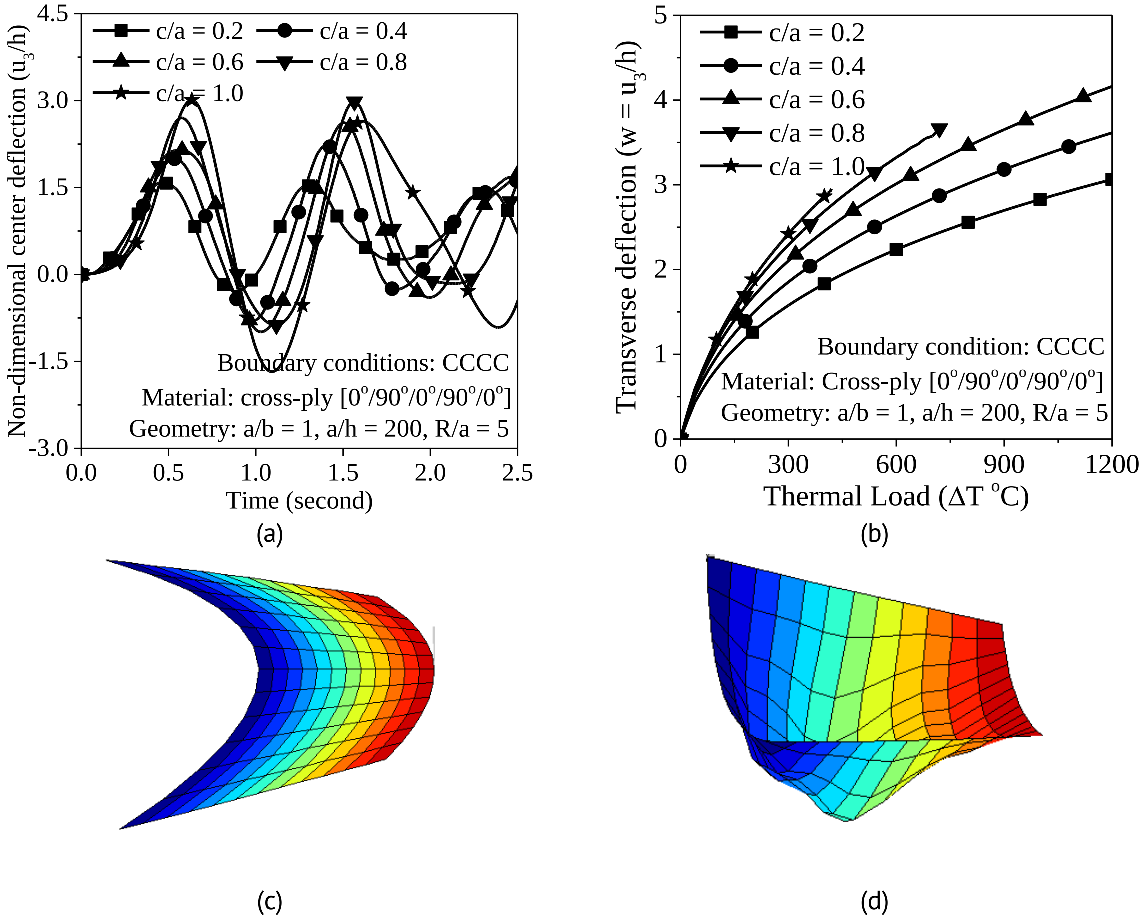

Fig. 5. Nonlinear static and dynamic response of clamped (*CCCC*) cross-ply [0°/90°/0°/90°/0°] composite trapezoidal panel (as given in Fig. 2(c)) under thermal environment (ΔT °C) considering various chord to span ratios: (a) nonlinear dynamic response at thermal load (ΔT =100 °C, at Room Temp. T_R = 20 °C); (b) nonlinear static response; (c) deformed shape of panel (c/a = 0.6) at time t = 0.563 second; (d) deformed shape of panel (c/a = 0.6) at time t = 1.034 second

Effect of boundary conditions on nonlinear dynamic response. Further, the effect of various boundary conditions such as: *CCCC*, *CSCS*, *SSSS* case 2 and *SCSF* has been investigated on nonlinear bending and transient responses of cross-ply [0°90°/0°/90°/0°] composite trapezoidal curved panels (a/b = 1, a/h = 200, c/a = 0.6 and R/a = 5) under thermal environment ΔT °C. The transient response of trapezoidal curved panel (R/a = 5, c/a = 0.6) under thermal load ΔT = 100 °C is presented in Fig. 6(a), whereas nonlinear bending response is given in Fig. 6(b) for various boundary conditions. It is noticed that thermal load carrying capacity of simply supported panel is much lower than the clamped trapezoidal panel. Also plotted the deformation shapes of trapezoidal curved panel at thermal load ΔT = 200 °C in Fig. 6 for various boundary conditions.

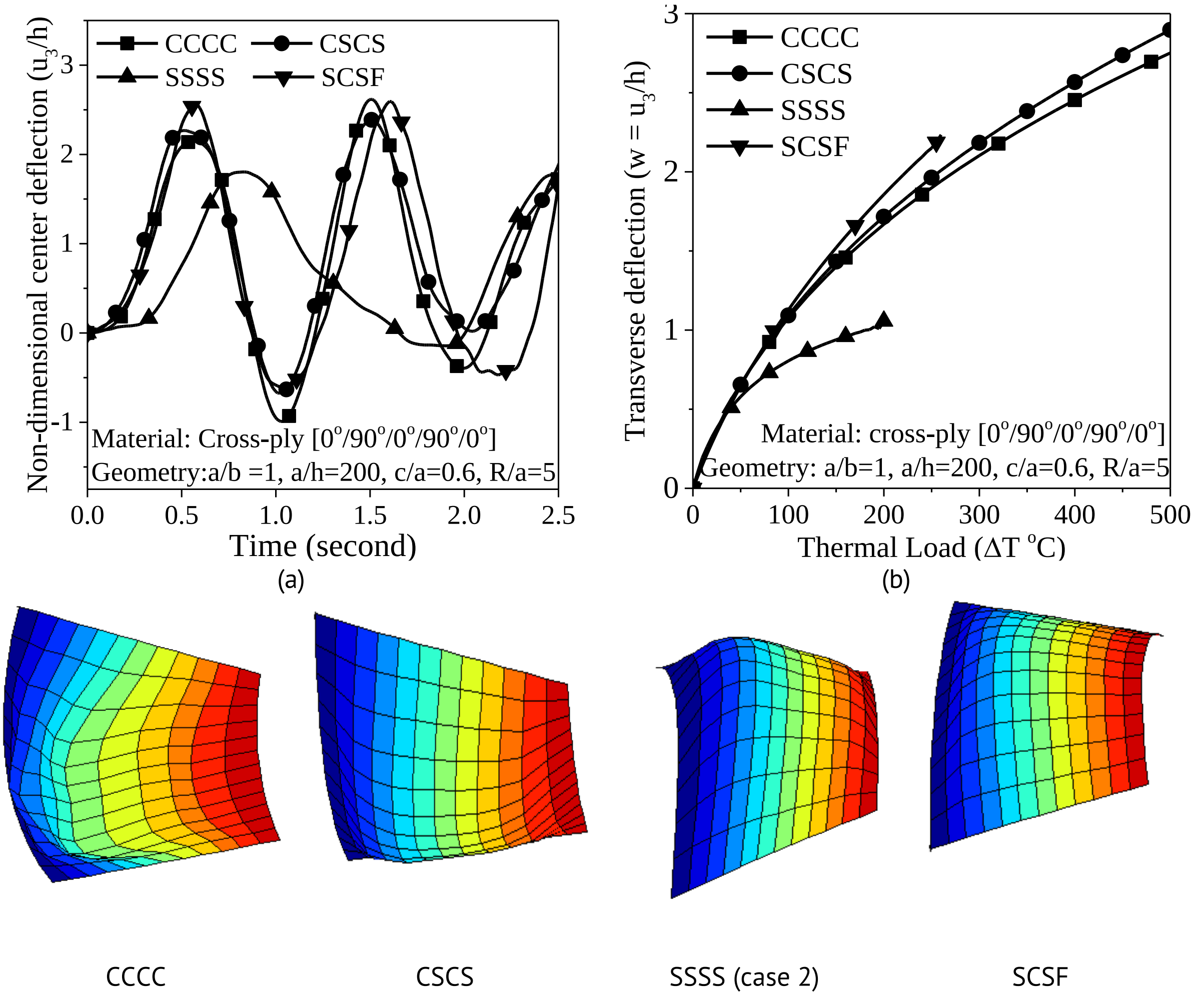

Fig. 6. Nonlinear dynamic and static response of cross-ply [0°/90°/0°/90°/0°] laminated composite trapezoidal curved panel under thermal load (ΔT °C at room temperature T_R = 20 °C) considering different boundary conditions with deformation shapes at ΔT = 200 °C

Nonlinear dynamic response under thermo-mechanical load. Next, studied the effect of intensity of thermal load (ΔT), cord-to-span ratio (c/a), radius-to-span ratio (R/a) and boundary conditions on the geometric nonlinear dynamic behaviour of fully clamped (*CCCC*) five-layered [45°/-45°/45°/-45°/45°] composite trapezoidal curved panel (a/b = 1, a/h = 200, h = 1) in presence of mechanical load (q_0 = 10 kN/m^2) ; and nonlinear dynamic response verses time is shown in Fig. 7. It is seen that by increasing intensity of thermal load from ΔT = 25 °C to 150 °C in the presence of constant radial pressure (q_0 = 10 kN/m^2) increases the non-dimensional transverse deformation u_3/h = 1.75 to 3.692 and time period of cycle is reduces from t = 1.382 second to 0.97 second as given in Fig. 7(a). Further, it is observed that by increasing the cord-to-span ratio (c/a) from 0.2 to 1.0 increases the non-dimensional central deflection (u_3/h) from 2.216 to 4.109, and structures vibration frequency reduces as the cyclic time increases from 0.926 second to 1.236 second as presented in Fig. 7(b) at thermal load (ΔT = 100 °C) and mechanical load (q_0 = 10 kN/m^2). Then, effect of radius-to-span ratio (R/a = 4, 5, 8, 10 and 12) changing from deep shell (R/a = 4) to shallow shell (R/a = 12) on nonlinear transient characteristics of angle-ply laminated trapezoidal curved panel subjected to thermal ΔT = 100 °C and mechanical load q_0 = 10 kN/m^2 is investigated in Fig. 7(c); it is found that trend of dynamic response is qualitatively similar as change in the cord to span ratios *c/a* = 0.2, to 1.0. Moreover, the same problem is investigated for fully clamped (CCCC), simply supported-clamped-free (SCSF), and simply supported (SSSS case 1 and SSSS case 2) composite trapezoidal curved panel subjected to thermal loading with radial pressure. The transient response of a symmetric trapezoidal cylindrical panel for four different boundary conditions is presented in Fig. 7(d).

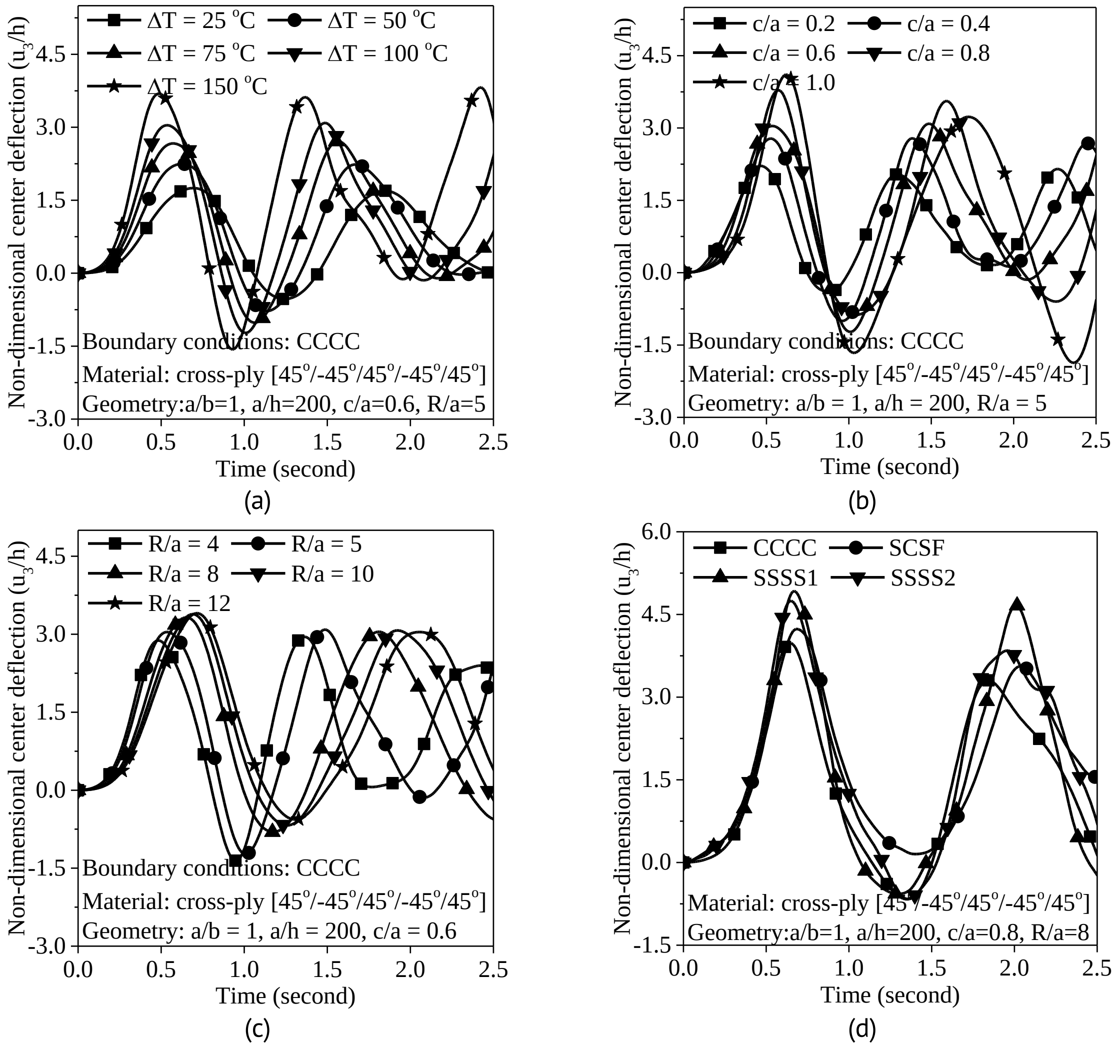

Fig. 7. Nonlinear dynamic response of angle-ply [45°/-45°/45°/-45°/45°] laminated composite trapezoidal curved panel to present the effect of (a) intensity of thermal load (ΔT °C), (b) cord to span ratio, (c) radius to span ratio and (d) boundary conditions considering four different cases in the presence of radial pressure q_0 = 10 kN/m^2

Conclusion

Geometrical nonlinear bending and flexural vibration characteristics of laminated composite trapezoidal curved panels are investigated here under thermal environment in the absence and presence of radial pressure. First, examined the accuracy of in-house FORTRAN code and validated the present numerical results of linear bending, linear vibration and geometric nonlinear dynamic response with available published results, it is found that, error is less than 0.02 percent or under the limit. Thereafter, new results for future research on the geometric nonlinear vibration characteristics of symmetric trapezoidal panels under thermal shock in the presence of mechanical load are presented. Here, investigated the effect of cord to span ratios (c/a), radius to span ratios (R/a), boundary conditions and stacking sequence on the nonlinear bending and dynamic response of composite trapezoidal cylindrical panels subjected to different heating rates (thermal shock loading) with and without mechanical load.

The vibration frequencies of trapezoidal cylindrical panel will increase with increase in intensity of thermal (ΔT = 25, 50, 75, 100 and 150 °C) and mechanical load (q_0 = 10 kN/m^2), whereas the vibration frequencies are of cross-ply and angle-ply laminated composite panels will reduce with increase in cord to span ratio from 0.2 to 1.0 and radius-to-span ratio (R/a = 4, 5, 8, 10 and 12); and magnitude of central deflection (u_3/h) is increase with incremental change is thermal load (ΔT); cord-to-span ratio; and radius-to-span ratio. This occurs due to reduction in structural stiffness of trapezoidal panel with incremental change in load intensity, cord-to-span ratio and radius-to-span ratio.

References

1. Srinivasan RS, Babu BJC. Free vibration and flutter of laminated quadrilateral plates. *Computers & Structures*. 1987;27(2): 297–304.

2. Saliba HT. Transverse free vibration of fully clamped symmetrical trapezoidal plates. *Journal of Sound and Vibration*. 126(2), 237–247.

3. Ng SSF, Das B. Free vibration and buckling analysis of clamped skew sandwich plates by the Galerkin method. *Journal of Sound and Vibration*. 1986;107(1): 97–106.

4. Qatu MS. Natural vibration of free, laminated composite triangular and trapezoidal shallow shells, *Composite Structures*. 1995;31(1): 9–19.

5. Han W, Petyt M. Linear vibration analysis of laminated rectangular plates using the hierarchical finite element method—I. Free vibration analysis. *Computers & Structures*. 1996;61(4): 705–712.

6. Han W, Petyt M. Linear vibration analysis of laminated rectangular plates using the hierarchical finite element method—II. Forced vibration analysis. *Computers & Structures*. 1996;61(4): 713–724.

7. Huang M, Ma XQ, Sakiyama T, Matsuda H, Morita C. Free vibration analysis of continuous rectangular plates. *Journal of Sound and Vibration*. 2010;329(4): 485–496.

8. Kumar A, Bhargava P, Chakrabarti A. Vibration of laminated composite skew hypar shells using higher order theory. *Thin-Walled Structures*. 2013;63: 82–90.

9. Malekzadeh P. A differential quadrature nonlinear free vibration analysis of laminated composite skew thin plates. *Thin-Walled Structures*. 2007;45(2): 237–250.

10. Gupta AK, Sharma S. Effect of thermal gradient on vibration of non-homogeneous orthotropic trapezoidal plate of linearly varying thickness. *Ain Shams Engineering Journal*. 2013;4(3): 523–530.

11. Nguyen-Minh N, Tran-Van N, Bui-Xuan T, Nguyen-Thoi T. Free vibration analysis of corrugated panels using homogenization methods and a cell-based smoothed Mindlin plate element (CS-MIN3). *Thin-Walled Structures*. 2018;124: 184–201.

12. Rout M, Hota SS, Karmakar A. Thermoelastic free vibration response of graphene reinforced laminated composite shells. *Engineering Structures*. 2019;178: 179–190.

13. Liu T, Wang Q, Qin B, Wang A. Free in-plane vibration of plates with arbitrary curvilinear geometry: Spectral-Chebyshev model and experimental study. *Thin-Walled Structures*. 2022;170: 108628.

14. Niu Y, Yao M. Linear and nonlinear vibrations of graphene platelet reinforced composite tapered plates and cylindrical panels. *Aerospace Science and Technology*. 2021;115: 106798.

15. Li C, Cheng H. Free vibration analysis of a rotating varying-thickness-twisted blade with arbitrary boundary conditions. *Journal of Sound and Vibration*. 2021;492: 115791.

16. Dou C, Jiang ZQ, Pi YL, Guo YL. Elastic shear buckling of sinusoidally corrugated steel plate shear wall. *Engineering Structures*. 2016;121: 136–146.

17. Franzoni F, Odermann F, Lanbans E, Bisagni C, Arbelo MA, Degenhardt R. Experimental validation of the vibration correlation technique robustness to predict buckling of unstiffened composite cylindrical shells. *Composite Structures*. 2019;224: 111107.

18. Magnucka-Blandzi E, Walczak Z, Jasion P, Wittenbeck L. Buckling and vibrations of metal sandwich beams with trapezoidal corrugated cores–the lengthwise corrugated main core. *Thin-Walled Structures*. 2017;112: 78–82.
19. Magnucka-Blandzi E, Walczak Z, Wittenbeck L, Jasion P, Rodak M, Szyc W, Lewiński J. Stability and vibrations of a metal seven-layer rectangular plate with trapezoidal corrugated cores. *Thin-Walled Structures*. 2017;114: 154–163.
20. Watts G, Kumar R, Patel SN, Singh S. Dynamic instability of trapezoidal composite plates under non-uniform compression using moving kriging based meshfree method. *Thin-Walled Structures*. 2021;164: 107766.
21. Kumari E, Lal S. Nonlinear Bending Analysis of Trapezoidal Panels under Thermo-Mechanical Load. *Forces in Mechanics*. 2022;8: 100097.
22. Kumari E, Saxena D. Buckling analysis of folded structures. *Materials Today: Proceedings*. 2021;43: 1421–1430.
23. Kumari E. Free vibration analysis of rotating laminated composite plate type blades with variable thickness. *Materials Today: Proceedings*. 2021;43: 1762–1773.
24. Kumari E. Dynamic response of composite panels under thermo-mechanical loading. *Journal of Mechanical Science and Technology*. 2022;36(8): 3781–3790.
25. Kumari E, Singha MK. Nonlinear response of laminated panels under blast load. *Procedia Engineering*. 2017;173: 539–546.
26. Kumari E, Singh J, Kasera G. Analysis of piston of internal combustion engine under thermo-mechanical load. *International Research Journal on Advanced Science Hub*. 2021;3: 11–18.
27. Sharma M, Kumari E, Meena PM. A parametric study to improve the heat transfer of solar air heater through CFD analysis. *Journal of Mechanical and Construction Engineering*. 2022;2: 1–17.
28. Kumar V, Singh SJ, Saran VH, Harsha SP. Vibration response of exponentially graded plates on elastic foundation using higher-order shear deformation theory. *Indian Journal of Engineering & Material Sciences*. 2022;29: 181–188.
29. Govindaraj T, Mahendran C, Manikandan VS, Archana J, Navaneethan M. Enhanced visible-light-driven photocatalytic activity of Ce doped WO3 nanorods for Rhodamine B dye degradation. *Materials Letters*. 2021;305: 130705.
30. Kumar A, Mariappan CR. A new biocompatible phosphate free mesoporous calcium borosilicate glass-ceramics for medical application. *Materials Letters*. 2021;305: 130752.
31. Panfilov P, Panfilov GP, Zaytsev D. Deformation behavior of polycrystalline rhenium under shear testing at room temperature. *Materials Letters*. 2020;277: 128379.
32. Myslyvchenko O, Bondar A, Petyukh V, Tikhonova I, Tsyganenko N. Structure of orthorhombic martensite in the Ti92. 5Nb5Mo2. 5 alloy, its deformation and thermal stability. *Materials Letters*. 2020;277: 128267.
33. Bathe KJ. *Finite Element Procedures*. Prentice-Hall of India; 1997.
34. Ko Y, Lee PS, Bathe KJ. The MITC+ shell element and its performance. *Computers & Structures*. 2016;169: 57–68.
35. Ko Y, Lee PS, Bathe KJ. The MITC+ shell element in geometric nonlinear analysis. *Computers & Structures*. 2017;185: 1–14.
36. Saadatpour MM, Azhari M. The Galerkin method for static analysis of simply supported plates of general shape. *Computers & Structures*. 1998;69(1): 1–9.
37. Maleki S, Tahani M. Non-linear analysis of moderately thick laminated plates and shell panels under thermo-mechanical loadings. *ZAMM-Journal of Applied Mathematics and Mechanics*. 2012;92(8): 652–667.
38. Chopra I, Durvasula S. Vibration of simply-supported trapezoidal plates I. Symmetric trapezoids. *Journal of Sound and Vibration*. 1971;19(4): 379–392.
39. Kitipornchai S, Xiang Y, Liew KM, Lim MK. A global approach for vibration of thick trapezoidal plates. *Computers & Structures*. 1994;53(1): 83–92.
40. Reddy JN, Chandrashekhara K. Geometrically non-linear transient analysis of laminated, doubly curved shells. *International Journal of Non-Linear Mechanics*. 1985;20(2): 79–90.
41. Bathe KJ. Conserving energy and momentum in nonlinear dynamics: a simple implicit time integration scheme. *Computers & Structures*. 2007;85(7-8): 437–445.

About Author

Kumari Emarti Sc
PhD, Assistant Professor (MBM University, Jodhpur, India)

Lal Shiv Sc
PhD, Associate Professor (Rajasthan Technical University, Kota, India)